Amirkabir Journal of Mechanical Engineering

Amirkabir J. Mech. Eng., 51(4) (2019) 1-4
DOI:

Thermal Performance and Entropy Generation Analysis of Nanofluid Flow in a Trapezoidal Heat Sink with Different Arrangements

H. Khorasanizadeh, M. Sepehrnia*

Mechanical Engineering and the Energy Research Institute, University of Kashan, Kashan, Iran

ABSTRACT: In this three dimensional numerical study, heat transfer characteristics and entropy generation of Alumina water nanofluid laminar flow in a trapezoidal micro channel heat sink have been investigated by considering conduction in solid parts for constant heat flux of 200 kW/m2 entering from the substrate. The governing equations have been solved using an element-based finite volume method. The main scope of this study has been investigating the effects of four horizontal entry/exit configurations (the A, B, C and D-type), from different parts of the entry and exit chambers, on heat transfer characteristics and entropy generation, whereas the effects of the Brownian motion of nanoparticles and temperature-dependent properties of the nanofluid are considered. The results show that for a constant volume fraction, increasing pressure drop increases the Nusselt number between 1.78% and 1.88%, but decreases the thermal resistance between 35.94% and 40.41%, the theta (temperature uniformity of substrate) between 33.90% and 41.60% and the total entropy generation between 24.34% and 27.15%. Also, for a constant pressure drop, increasing volume fraction from 0% to 4% increases the Nusselt number between 11.88% and 12.06% and the total entropy generation between 1.77% and 2.37% while it does not have impressive effect on thermal resistance and theta, so that with increasing the volume fraction the thermal resistance and theta changes are less than 1% and 2%, respectively. The highest increase of the total entropy generation, with increasing the volume fraction from 0% to 4%, is 2.37% for the A-type and the lowest is 1.77% for the D-type. From thermodynamics second law point of view and because of the lower total entropy generation, at low pressure drop of 5 kPa the B-type and at high pressure drops of 10 kPa and 15 kPa the C-type are the best arrangements but from the thermal indexes point of view the A-type is always better than other arrangements.

Review History:
Received:
Revised:
Accepted:
Available Online:

Keywords:
Thermal performance
Entropy generation
Microchannel
Different arrangement
Nanofluid

1- Introduction

The minimization of entropy generation is a way to reduce the irreversibility of fluid flow and heat transfer. Singh et al. [1] investigated entropy generation and heat transfer of Al_2O_3-water nanofluid flow in a microchannel, a minichannel and a channel. Their results showed that using the nanofluid increases entropy generation. Mah et al. [2] investigated the effect of viscous dissipation in the laminar and fully developed Al_2O_3-water nanofluid flow in a circular microchannel analytically and showed it affects the temperature distribution. Sohel et al. [3] numerically studied entropy generation in a microchannel and a minichannel using nanofluid. They observed entropy generation decreases with increasing the nanoparticles volume fraction. Pourmahmoud et al. [4] studied heat transfer, entropy generation and fluid flow in the ribbed microchannel, numerically. They found that frictional irreversibility increases when the rib height increases. Leong and Ong [5] studied entropy generation of nanofluid flow in microchannels with circle, square and equilateral triangle cross sections. They observed that circular microchannel has the minimum entropy generation in comparison with the other two.

The trapezoidal geometry is used in the casting industry and cooling of electronic chips that are placed in an unwanted space. Thermal performance and entropy generation due to nanofluid flow in a trapezoidal Micro Channel Heat Sink (MCHS) for different entry/exit arrangements have not been studied so far, therefore in this study they are considered. For analyzing the heat sink performance, in addition to three common indexes utilized in the previous research works (average Nusselt number, thermal resistance and theta) entropy generation is also used.

2- Problem Description

The dimension details of the A-type arrangement are shown in Fig. 1. The location of the flow entry and exit for the other three heat sink types are shown in Fig. 2. The dimensions of microchannels and fins and the microchannel numbers are shown in Fig. 3.

3- Governing Equations and Performance Indexes

The continuity equation, momentum equations in three directions x, y and z, and also energy balances in the fluid and solid part are respectively:

$$\frac{\partial}{\partial x}(\rho_{eff}u)+\frac{\partial}{\partial y}(\rho_{eff}v)+\frac{\partial}{\partial z}(\rho_{eff}w)=0 \quad (1)$$

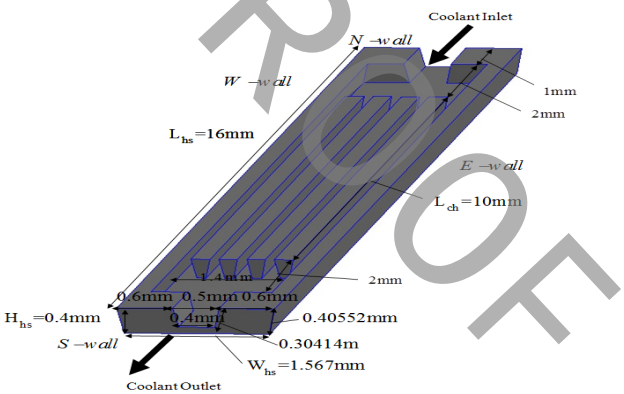

Fig. 1. Geometry of A-type microchannel heat sink with direct entry and exit.

Corresponding author, E-mail: msepehr_91@yahoo.com

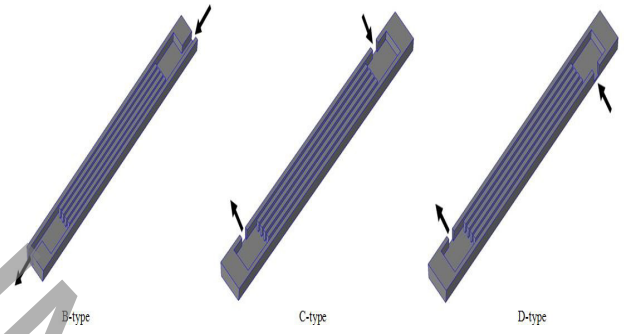

Fig. 2. The geometry of the B-, C- and D-type entry/exit arrangement.

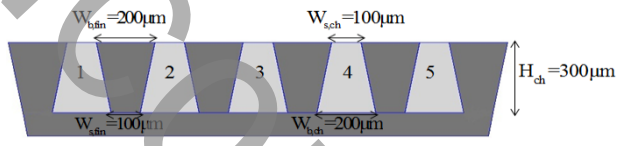

Fig. 3. Fin and microchannel dimensions.

$$\frac{\partial}{\partial x}\left(\rho_{eff}uu\right)+\frac{\partial}{\partial y}\left(\rho_{eff}vu\right)+\frac{\partial}{\partial z}\left(\rho_{eff}wu\right)= -\frac{\partial p}{\partial x}+\frac{\partial}{\partial x}\left(\mu_{eff}\frac{\partial u}{\partial x}\right)+\frac{\partial}{\partial y}\left(\mu_{eff}\frac{\partial u}{\partial y}\right)+\frac{\partial}{\partial z}\left(\mu_{eff}\frac{\partial u}{\partial z}\right) \quad (2)$$

$$\frac{\partial}{\partial x}\left(\rho_{eff}uv\right)+\frac{\partial}{\partial y}\left(\rho_{eff}vv\right)+\frac{\partial}{\partial z}\left(\rho_{eff}wv\right)= -\frac{\partial p}{\partial y}+\frac{\partial}{\partial x}\left(\mu_{eff}\frac{\partial v}{\partial x}\right)+\frac{\partial}{\partial y}\left(\mu_{eff}\frac{\partial v}{\partial y}\right)+\frac{\partial}{\partial z}\left(\mu_{eff}\frac{\partial v}{\partial z}\right) \quad (3)$$

$$\frac{\partial}{\partial x}\left(\rho_{eff}uw\right)+\frac{\partial}{\partial y}\left(\rho_{eff}vw\right)+\frac{\partial}{\partial z}\left(\rho_{eff}ww\right)= -\frac{\partial p}{\partial z}+\frac{\partial}{\partial x}\left(\mu_{eff}\frac{\partial w}{\partial x}\right)+\frac{\partial}{\partial y}\left(\mu_{eff}\frac{\partial w}{\partial y}\right)+\frac{\partial}{\partial z}\left(\mu_{eff}\frac{\partial w}{\partial z}\right) \quad (4)$$

$$\frac{\partial}{\partial x}\left(\rho_{eff}uT\right)+\frac{\partial}{\partial y}\left(\rho_{eff}vT\right)+\frac{\partial}{\partial z}\left(\rho_{eff}wT\right)= \frac{\partial}{\partial x}\left(\frac{k_{eff}}{c_{p,eff}}\frac{\partial T}{\partial x}\right)+\frac{\partial}{\partial y}\left(\frac{k_{eff}}{c_{p,eff}}\frac{\partial T}{\partial y}\right)+\frac{\partial}{\partial z}\left(\frac{k_{eff}}{c_{p,eff}}\frac{\partial T}{\partial z}\right) \quad (5)$$

$$\frac{\partial}{\partial x}\left(k_s\frac{\partial T}{\partial x}\right)+\frac{\partial}{\partial y}\left(k_s\frac{\partial T}{\partial y}\right)+\frac{\partial}{\partial z}\left(k_s\frac{\partial T}{\partial z}\right)=0 \quad (6)$$

Four performance indexes of average Nusselt number, thermal resistance, theta and entropy generation are:

$$Nu=\frac{\bar{h}D_h}{k_f} \quad (7)$$

$$R_{th}=\frac{T_{w,\max}-T_{in}}{q_w W_{hs} L_{hs}} \quad (8)$$

$$\theta=\frac{T_{b,\max}-T_{b,\min}}{q_w} \quad (9)$$

$$S=\frac{k_{eff}}{T_f^2}\left[\left(\frac{\partial T_f}{\partial x}\right)^2+\left(\frac{\partial T_f}{\partial y}\right)^2+\left(\frac{\partial T_f}{\partial z}\right)^2\right]+ \frac{k_s}{T_s^2}\left[\left(\frac{\partial T_s}{\partial x}\right)^2+\left(\frac{\partial T_s}{\partial y}\right)^2+\left(\frac{\partial T_s}{\partial z}\right)^2\right]+ \frac{\mu_{eff}}{T_f^2}\left\{\begin{array}{l}2\left[\left(\frac{\partial u}{\partial x}\right)^2+\left(\frac{\partial v}{\partial y}\right)^2+\left(\frac{\partial w}{\partial z}\right)^2\right]+\\ \left(\frac{\partial u}{\partial y}+\frac{\partial v}{\partial x}\right)^2+\left(\frac{\partial v}{\partial z}+\frac{\partial w}{\partial y}\right)^2+\left(\frac{\partial w}{\partial x}+\frac{\partial u}{\partial z}\right)^2\end{array}\right\} \quad (10)$$

Table 1. Performance indexes of the MCHS with various entry/exit arrangements for different pressure drops but volume fraction of 4%.

ΔP (kPa)	Index	A	B	C	D
5	Nu	24.98	24.58	24.05	24.19
	Relative differ-ence (%)	-	1.60	3.72	3.16
10	Nu	25.17	24.76	24.17	24.34
	Relative differ-ence (%)	-	1.63	3.97	3.30
15	Nu	25.45	25.04	24.49	24.62
	Relative differ-ence (%)	-	1.61	3.77	3.26
5	R_{th}	4.19	4.33	5.62	6.12
	Relative differ-ence (%)	-	3.34	34.13	46.06
10	R_{th}	3.07	3.09	3.97	4.46
	Relative differ-ence (%)	-	0.65	29.31	45.27
15	R_{th}	2.56	2.58	3.60	3.76
	Relative differ-ence (%)	-	0.78	40.62	46.87
5	Θ	7.43E-5	7.74E-5	10.6E-5	11.9E-5
	Relative differ-ence (%)	-	4.17	43.34	60.07
10	Θ	5.40E-5	5.45E-5	7.57E-5	8.79E-5
	Relative differ-ence (%)	-	0.92	40.18	62.78
15	Θ	4.48E-5	4.52E-5	7.04E-5	7.44E-5
	Relative differ-ence (%)	-	0.89	57.14	66.07
5	S_{tot}	4690.55	4499.26	4555.0	4807.25
	Relative differ-ence (%)	4.25	-	1.24	6.84
10	S_{tot}	3810.50	3745.85	3661.6	3920.97
	Relative differ-ence (%)	4.06	2.30	-	7.08
15	S_{tot}	3416.97	3404.17	3362.1	3580.59
	Relative differ-ence (%)	1.63	1.25	-	6.50

4- Results and Discussion

The results for the four performance indexes have been presented in Table 1. As noticed from Table 1, for all of the pressure drops in terms of the average Nusselt number the A, B, D and C-type MCHS have the best performance, respectively. Also from thermal resistance and theta point of views the A, B, C and D-type MCHS have the best performance, respectively. From entropy generation point of view, for the pressure drop of 5 kPa, the B-type MCHS has the best performance followed by the C, A and D-type, respectively. For the pressure drops of 10 and 15 kPa, the C- type has the best performance followed by the B, A and D-type, respectively.

5- Conclusions

Numerical results showed that with increasing pressure drop from 5 to 15 kPa, the average Nusselt number increases between 1.78% and 1.88%, thermal resistance decreases between 35.94% and 40.41%, theta decreases between 33.90% and 41.60%, and total entropy generation decreases between 24.34% and 27.15%. In overall results showed that the A-type arrangement is the best.

References

[1] P. K. Singh, K. Anoop, T. Sundararajan, and S. K. Das, "Entropy generation due to flow and heat transfer in nanofluids," International Journal of Heat and Mass Transfer, vol. 53, pp. 4757-4767, 2010.

[2] W. H. Mah, Y. M. Hung, and N. Guo, "Entropy generation of viscous dissipative nanofluid flow in microchannels," International Journal of Heat and Mass Transfer, vol. 55, pp. 4169-4182, 2012.

[3] M. Sohel, R. Saidur, N. Hassan, M. Elias, S. Khaleduzzaman, and I. Mahbubul, "Analysis of entropy generation using nanofluid flow through the circular microchannel and minichannel heat sink," International Communications in Heat and Mass Transfer, vol. 46, pp. 85-91, 2013.

[4] N. Pourmahmoud, H. Soltanipour, and I. Mirzaee, "The effects of longitudinal ribs on entropy generation for laminar forced convection in a microchannel," Thermal Science, pp. 110-110, 2014.

[5] K. Leong and H. C. Ong, "Entropy generation analysis of nanofluids flow in various shapes of cross section ducts," International Communications in Heat and Mass Transfer, vol. 57, pp. 72-78, 2014.

Please cite this article using:

H. Khorasanizadeh and M. Sepehrnia, Thermal Performance and Entropy Generation Analysis of Nanofluid Flow in a Trapezoidal Heat Sink with Different Arrangements, *Amirkabir J. Mech. Eng.*, 51(4) (2019) 1-4.

DOI: